



Short communication

## Fabrication of all-solid-state lithium battery with lithium metal anode using Al<sub>2</sub>O<sub>3</sub>-added Li<sub>7</sub>La<sub>3</sub>Zr<sub>2</sub>O<sub>12</sub> solid electrolyte

Masashi Kotobuki<sup>a</sup>, Kiyoshi Kanamura<sup>a,\*</sup>, Yosuke Sato<sup>b</sup>, Toshihiro Yoshida<sup>b</sup><sup>a</sup> Department of Applied Chemistry, Graduate School of Urban Environmental Science, Tokyo Metropolitan University, 1-1 Minami-Ohsawa, Hachioji, Tokyo 192-0397, Japan<sup>b</sup> NGK Insulators, Ltd., 2-56 Suda-cho, Mizuho, Nagoya, Aichi 467-8530, Japan

## ARTICLE INFO

## Article history:

Received 8 January 2011

Received in revised form 6 April 2011

Accepted 21 April 2011

Available online 29 April 2011

## Keywords:

All-solid-state Li ion battery

Solid electrolyte

Lithium battery

Li metal anode

## ABSTRACT

Li<sub>7</sub>La<sub>3</sub>Zr<sub>2</sub>O<sub>12</sub> (LLZ) solid electrolyte is one of the promising electrolytes for all-solid-state battery due to its high Li ion conductivity and stability against Li metal anode. However, high calcination temperature for LLZ preparation promotes formation of La<sub>2</sub>Zr<sub>2</sub>O<sub>7</sub> impurity phase. In this paper, an effect of Al<sub>2</sub>O<sub>3</sub> addition as sintering additive on LLZ solid electrolyte preparation and electrochemical properties of Al<sub>2</sub>O<sub>3</sub>-added LLZ were examined. By the Al<sub>2</sub>O<sub>3</sub> addition, sintered LLZ pellet could be obtained after 1000 °C calcination, which is 230 °C lower than that without Al<sub>2</sub>O<sub>3</sub> addition. Chemical and electrochemical properties of the Al<sub>2</sub>O<sub>3</sub>-added LLZ, such as stability against Li metal and ion conductivity, were comparable with the LLZ without Al<sub>2</sub>O<sub>3</sub> addition, i.e.  $\sigma_{\text{bulk}}$  and  $\sigma_{\text{total}}$  were  $2.4 \times 10^{-4}$  and  $1.4 \times 10^{-4}$  S cm<sup>-1</sup> at 30 °C, respectively. All-solid-state battery with Li/Al<sub>2</sub>O<sub>3</sub>-added LLZ/LiCoO<sub>2</sub> configuration was fabricated and its electrochemical properties were tested. In cyclic voltammogram, clear redox peaks were observed, indicating that the all-solid-state battery with Li metal anode was successfully operated. The redox peaks were still observed even after one year storage of the all-solid-state battery in the Ar-filled globe-box. It can be inferred that the Al<sub>2</sub>O<sub>3</sub>-added LLZ electrolyte would be a promising candidate for all-solid-state battery because of facile preparation by the Al<sub>2</sub>O<sub>3</sub> addition, relatively high Li ion conductivity, and good stability against Li metal and LiCoO<sub>2</sub> cathode.

© 2011 Elsevier B.V. All rights reserved.

### 1. Introduction

In current information-rich society, rechargeable lithium ion batteries are a key component [1]. They have been widely used as energy sources for a variety of electronic devices such as mobile phones and laptop computers because of their high energy densities [2]. However, fast progress of the electronic device has required further improvement of energy density of the lithium ion batteries [3].

Li metal anode has the largest capacity in all anode materials due to no need for any matrix components, 3862 mA h g<sup>-1</sup> [4], that is 10 times larger than that of present graphite anode (372 mA h g<sup>-1</sup> [5]). Therefore, the Li metal anode can satisfy a requirement for energy density improvement. However, a successful development of Li metal anode has not been achieved yet, because dendritic growth of Li metal during charge–discharge cycles makes a short circuit and finally causes safety problems like fire hazards [6]. All-solid-state Li battery with ceramics electrolyte can suppress the dendritic growth of Li metal and has been considered as a promising battery for next generation high performance power sources

[7,8]. However, most of good Li ion conductive ceramics such as Li<sub>0.35</sub>La<sub>0.55</sub>TiO<sub>3</sub> (LLT) and Li<sub>1.5</sub>Al<sub>0.5</sub>Ti<sub>1.5</sub>(PO<sub>4</sub>)<sub>3</sub> contain Ti which is instable against Li metal by facile reduction of Ti<sup>4+</sup> in contact with Li metal [9].

Recently, Li<sub>7</sub>La<sub>3</sub>Zr<sub>2</sub>O<sub>12</sub> (LLZ) with garnet-like structure was discovered as a novel family of fast lithium ion conductor that possesses enough high Li ion conductivity for practical all-solid-state battery [10]. This material has been much attention because of its chemical stability against Li metal. This new finding indicates that the all-solid-state battery with Li metal anode can be fabricated. We have minutely tested an availability of LLZ as a solid electrolyte for the all-solid-state battery and succeeded on operation of Li/LLZ/LiCoO<sub>2</sub> cell [11]. However, LLZ preparation requires high temperature calcination (1230 °C) which causes an easy formation of La<sub>2</sub>Zr<sub>2</sub>O<sub>7</sub> impurity. The formation of La<sub>2</sub>Zr<sub>2</sub>O<sub>7</sub> impurity should be avoided because the impurity reduces Li ion conductivity. Therefore, lowering calcination temperature and/or new preparation method has been required. We propose on usage of sintering additive to decrease calcination temperature.

Herein, we report an effect of Al<sub>2</sub>O<sub>3</sub> addition as the sintering additive on LLZ preparation and electrochemical properties of Al<sub>2</sub>O<sub>3</sub>-added LLZ. Additionally, successful operation of all-solid-state battery with Li metal anode that is Li/Al<sub>2</sub>O<sub>3</sub>-added LLZ/LiCoO<sub>2</sub> configuration is also reported.

\* Corresponding author. Tel.: +81 42 677 2828, fax: +81 42 677 2828.  
E-mail address: [kanamura@tmu.ac.jp](mailto:kanamura@tmu.ac.jp) (K. Kanamura).

## 2. Experimental

$\text{Li}_7\text{La}_3\text{Zr}_2\text{O}_{12}$  (LLZ) was prepared by a solid-state reaction.  $\text{LiOH}$  (Kanto Kagaku)  $\text{La}(\text{OH})_3$  (Shinetsu kagaku) and  $\text{ZrO}_2$  (TOHSO) (molar ratio = 7:3:2) were mixed in agate mortar and then calcined at  $900^\circ\text{C}$  for 6 h. 1.25 mol% of  $\gamma\text{-Al}_2\text{O}_3$  (Daimei Kagaku) was added to the obtained LLZ powder. The  $\text{Al}_2\text{O}_3$ -added powder was pelletized into a pellet with 13 mm diameter and then calcined at  $900\text{--}1100^\circ\text{C}$  for 36 h. After calcination, the pellets were polished to obtain flat surface and to control its thickness to 1 mm.

An observation of cross section of the pellet was performed by scanning electron microscope (SEM, JEOL). XRD (RINT-Ultima, Rigaku) was used for identification of crystal phases of the pellet using  $\text{Cu K}\alpha$  radiation.

Li ion conductivity of the pellet was examined by the AC impedance method with SI1260 impedance/gain-phase analyzer (Solartron analytical). Prior to measure, Au was sputtered on both sides of the pellet to ensure electrical contact. Data were collected at  $\pm 5$  mV voltage signal in a frequency range of 1 Hz–1 MHz using as-prepared cells at OCV at temperature range of  $30\text{--}220^\circ\text{C}$ .

Stability of the pellet against molten Li metal was tested by contact of the pellet with molten Li on Ni plate in Ar-filled globe box. After contact for 72 h, the pellet was removed from the molten Li and supplied for XRD measurement.

A cyclic voltammetry (CV) was measured using Li/LLZ/Au configuration to check electrochemical window of the pellet. To obtain better contact between LLZ pellet and Li metal, the pellet was put on the molten Li with 5 mm diameter in the globe box. The measurement was performed using HSV-100 (Hokuto denko) electrochemical analyzer in the range of  $-0.5$  to  $5$  V vs.  $\text{Li}/\text{Li}^+$  at scan rate of  $10$  mV  $\text{min}^{-1}$  at room temperature.

$\text{LiCoO}_2$  cathode with  $3\ \mu\text{m}$  thickness was prepared on the pellet by Magnetron sputtering under 30%  $\text{O}_2/\text{Ar}$  atmosphere at substrate temperature of  $500^\circ\text{C}$ . The sputtered  $\text{LiCoO}_2$  was characterized XRD and Raman (NRS-1000, JASCO) with 532 nm laser radiation. Then, all-solid-state battery with Li/LLZ/ $\text{LiCoO}_2$  configuration was fabricated by putting Li metal on bare side of  $\text{LiCoO}_2/\text{LLZ}$  pellet. The CV measurement of the all-solid-state battery was performed at scan rate of  $1$  mV  $\text{min}^{-1}$  with scan range of  $3.3\text{--}4.2$  V vs.  $\text{Li}/\text{Li}^+$  at room temperature.

## 3. Results

The  $\text{Al}_2\text{O}_3$ -added LLZ pellet was calcined at various temperatures. Cross-sectional SEM images of the pellets are shown in Fig. 1. In the pellet calcined at  $900^\circ\text{C}$  (Fig. 1(a)), many grains were observed. These many grains make us image that the pellet possesses high grain boundary resistance derived by much number of grain boundaries. The pellet sintered well with increasing calcination temperature. Finally, no grain boundary was observed in cross section of the pellet calcined at  $1100^\circ\text{C}$  (Fig. 1(c)). Some voids existed in the cross-sectional view of the pellet calcined at  $1100^\circ\text{C}$  (Fig. 1(c)), but it can be confirmed that they were isolated sufficiently to prevent electrical short circuit in rechargeable lithium batteries. It is expected that the void formation can be reduced by using smaller LLZ particles for the pellet preparation.

XRD patterns of LLZ pellets calcined at  $900\text{--}1100^\circ\text{C}$  were depicted in Fig. 2. In  $900$  and  $1000^\circ\text{C}$  calcination, the XRD patterns were well-matched with the standard pattern known as a garnet phase  $\text{Li}_5\text{La}_3\text{Nb}_2\text{O}_{12}$  (PDF 45-0109), indicating that LLZ with garnet-like structure was prepared [10]. No diffraction peak from  $\text{Al}_2\text{O}_3$  was observed. With increase of calcination temperature, the diffraction peaks became sharper. Formation of impurity phase of pyrocholate  $\text{La}_2\text{Zr}_2\text{O}_7$  was confirmed in the pellet calcined at  $1100^\circ\text{C}$ . From these results, it is concluded that optimum calci-

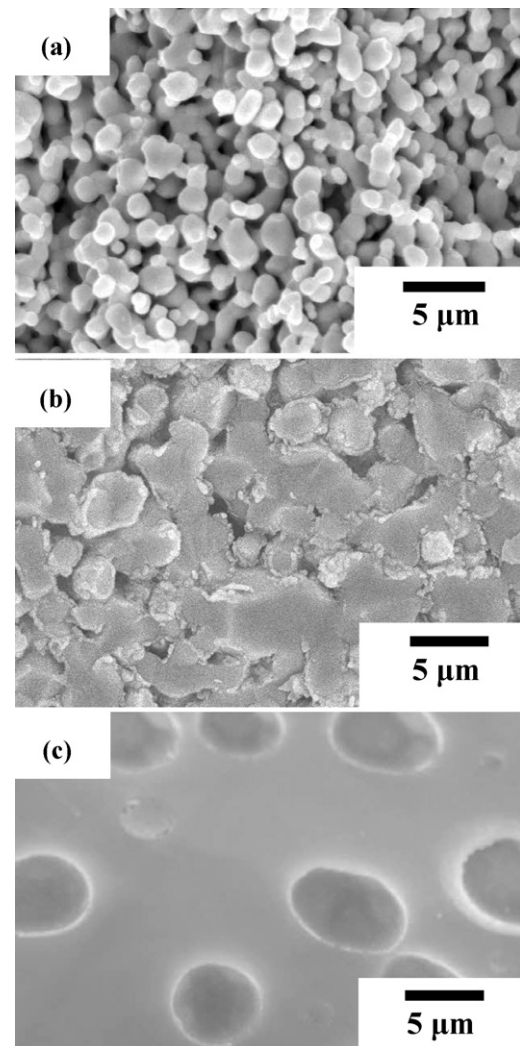


Fig. 1. Cross-sectional SEM images of  $\text{Al}_2\text{O}_3$ -added LLZ pellet calcinated at (a)  $900^\circ\text{C}$ , (b)  $1000^\circ\text{C}$ , and (c)  $1100^\circ\text{C}$  for 36 h.

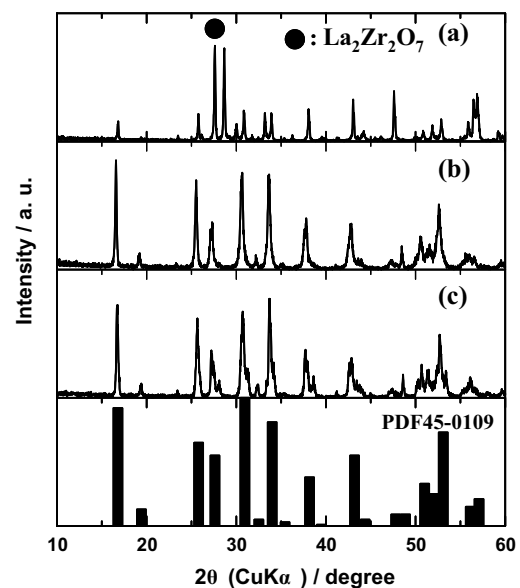


Fig. 2. XRD patterns of  $\text{Al}_2\text{O}_3$ -added LLZ pellet calcinated at (a)  $1100^\circ\text{C}$ , (b)  $1000^\circ\text{C}$ , and (c)  $900^\circ\text{C}$  for 36 h.

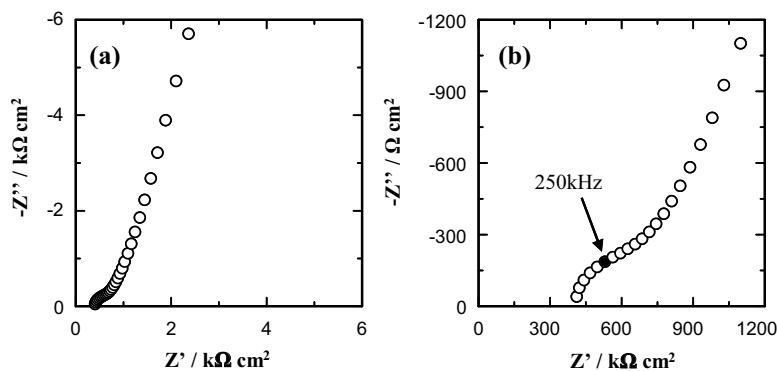


Fig. 3. Complex impedance plot of  $\text{Al}_2\text{O}_3$ -added LLZ pellet calcined at  $1000^\circ\text{C}$ . (a) Whole plot and (b) magnified plot around origin. Measurement was performed at  $30^\circ\text{C}$ .

nation temperature for  $\text{Al}_2\text{O}_3$ -added LLZ pellet is  $1000^\circ\text{C}$ . This calcination temperature is  $230^\circ\text{C}$  lower than that of LLZ without  $\text{Al}_2\text{O}_3$  addition [10,11].

A complex impedance plot of the  $\text{Al}_2\text{O}_3$ -added LLZ pellet calcined at  $1000^\circ\text{C}$  using blocking Au electrodes is revealed in Fig. 3. A semicircle and Warburg-type impedance were appeared at high frequency and low frequency regions, respectively. This tail at low frequencies corresponds to a usual behavior of ionically blocking electrodes with ionically conductive nature [12]. A similar behavior has been observed another garnet-like ceramic conductor [13–17].  $\sigma_{\text{bulk}}$  and  $\sigma_{\text{total}}$  estimated from intercepts of the semicircle at high and low frequency sides were  $2.4 \times 10^{-4}$  and  $1.4 \times 10^{-4} \text{ S cm}^{-1}$ , respectively. These are comparable with reported value by Weppner et al. [10]. The Arrhenius plot of bulk conductivity of  $\text{Al}_2\text{O}_3$ -added LLZ pellet in the temperature range of  $30$ – $220^\circ\text{C}$  was shown in Fig. 4. The plot was fit by a straight line, indicating that ion conductive mechanism of the  $\text{Al}_2\text{O}_3$ -added LLZ is identical in this temperature range. Estimated activation energy from a slope of the line was  $0.35 \text{ eV}$  which is close to the reported value of  $0.31 \text{ eV}$  [10].

In order to test a stability of the  $\text{Al}_2\text{O}_3$ -added LLZ against Li metal, the LLZ pellet was put on melting Li metal for 72 h. No visual change of the LLZ pellet was confirmed by photos of LLZ before and after contact with Li metal (Fig. 5). XRD patterns of them were also completely identical and new diffraction peaks did not appear (Fig. 6), indicating that the  $\text{Al}_2\text{O}_3$ -added LLZ was stable against Li metal. The  $\text{Al}_2\text{O}_3$ -addition did not affect on stability of the LLZ against Li metal.

A cyclic voltammetry (CV) of  $\text{Li}/\text{Al}_2\text{O}_3$ -added LLZ/Au cell was measured to check electrochemical window of the  $\text{Al}_2\text{O}_3$ -added LLZ. Peaks due to formation of Au–Li alloy and extraction of Li from the alloy were clearly observed, indicating that lithium ion could

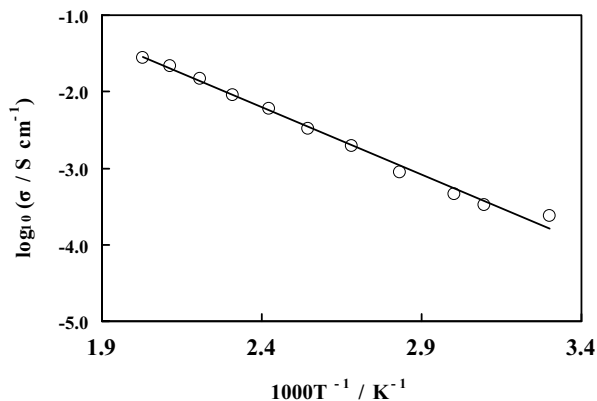


Fig. 4. Arrhenius plot of bulk Li ion conductivity of  $\text{Al}_2\text{O}_3$ -added LLZ pellet calcined at  $1000^\circ\text{C}$  in the temperature range of  $30$ – $220^\circ\text{C}$ .

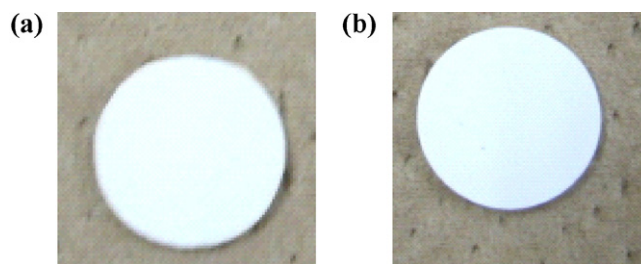


Fig. 5. Photos of  $\text{Al}_2\text{O}_3$ -added LLZ pellet calcined at  $1000^\circ\text{C}$  (a) before and (b) after contact with molten Li metal for 72 h.

be transferred through the LLZ electrolyte without any degradation of LLZ. At anodic potential side, the LLZ was stable until 5 V. This nature implies that high voltage cathode material, such as  $\text{LiCoPO}_4$  and  $\text{LiNi}_{0.5}\text{Mn}_{1.5}\text{O}_4$ , can be applied to all-solid-state battery with LLZ solid electrolyte and fabrication of 5 V class batteries is possible (Fig. 7).

All-solid-state battery with Li metal anode using  $\text{Al}_2\text{O}_3$ -added LLZ solid electrolyte was fabricated by using  $\text{LiCoO}_2$  cathode. The  $\text{LiCoO}_2$  cathode with about  $3 \mu\text{m}$ -thickness on the  $\text{Al}_2\text{O}_3$ -added LLZ was prepared by sputtering. XRD pattern revealed oriented deposition of  $\text{LiCoO}_2$  on the LLZ, a sharp diffraction peak from (003) of  $\text{LiCoO}_2$  was observed (Fig. 8). All other peaks were attributed to LLZ and no impurity phase was detected. In Raman spectrum, weak Raman band was confirmed at  $594 \text{ cm}^{-1}$  (Fig. 9). This band may be attributed to HT- $\text{LiCoO}_2$  with hexagonal layered structure [18] which is favourable structure for cathode of lithium

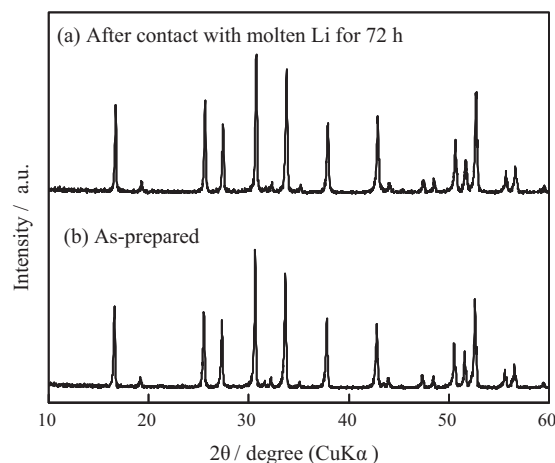


Fig. 6. XRD patterns of  $\text{Al}_2\text{O}_3$ -added LLZ pellet calcined at  $1000^\circ\text{C}$  (a) after and (b) before contact with molten Li metal for 72 h.

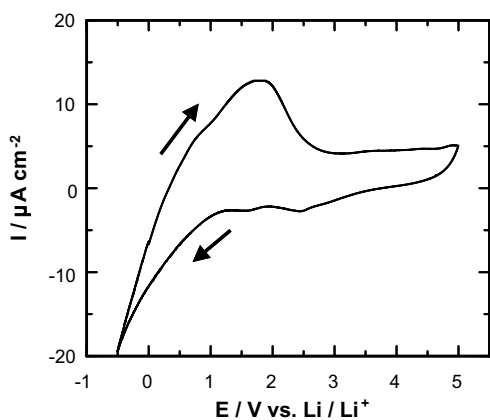


Fig. 7. Cyclic voltammogram of Li/Al<sub>2</sub>O<sub>3</sub>-added LLZ/Au cell at scan rate of 10 mV min<sup>-1</sup> in the potential range from -0.5 to 5 V vs. Li/Li<sup>+</sup>.

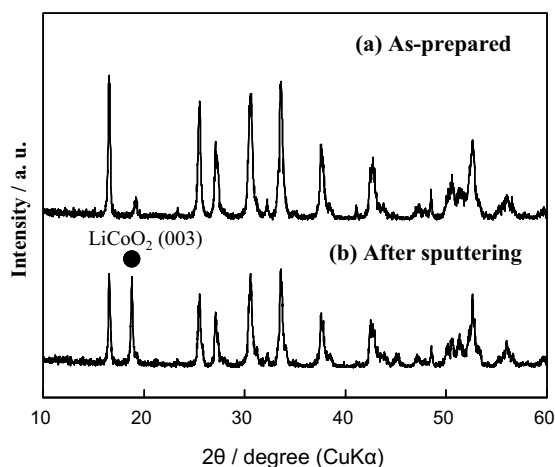


Fig. 8. XRD patterns of Al<sub>2</sub>O<sub>3</sub>-added LLZ pellet calcined at 1000 °C (a) before and (b) after LiCoO<sub>2</sub> sputtering.

battery [19]. All-solid-state battery composed of Li/Al<sub>2</sub>O<sub>3</sub>-added LLZ/LiCoO<sub>2</sub> configuration was fabricated by setting Li metal on bare side of LiCoO<sub>2</sub>/LLZ pellet and was supplied to CV measurement. The cyclic voltammogram was shown in Fig. 10(a). In an anode scan, oxidation peak was observed around at 3.9–4.2 V vs. Li/Li<sup>+</sup> which corresponded to some structure changes of LiCoO<sub>2</sub> [19,20]. There is no doubt that deintercalation of Li ion from LiCoO<sub>2</sub> on the LLZ and deposition of Li in the Li metal anode side are proceeding during the anode scan. In cathode scan, a reduction peak was

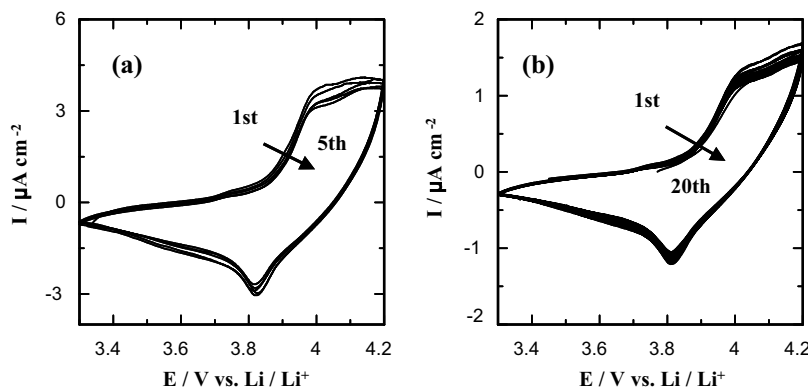


Fig. 10. Cyclic voltammograms of Li/Al<sub>2</sub>O<sub>3</sub>-added LLZ/LiCoO<sub>2</sub> cell (a) just after fabrication and (b) after preservation in Ar-filled globe box for one year at scan rate of 1 mV min<sup>-1</sup>.

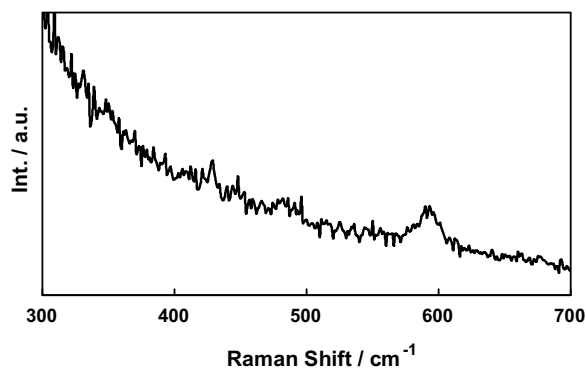


Fig. 9. Raman spectrum of Al<sub>2</sub>O<sub>3</sub>-added LLZ pellet calcined at 1000 °C after LiCoO<sub>2</sub> sputtering.

appeared as well. It is concluded that the all-solid-state battery with Li metal anode is operated successfully by using the Al<sub>2</sub>O<sub>3</sub>-added LLZ electrolyte. Both anodic and cathodic peak current densities were about 3 μA cm<sup>-2</sup>. In order to check long-term storage property, CV measurement of the Li/LLZ/LiCoO<sub>2</sub> cell was performed after the cell was preserved in Ar-filled glove box for one year (Fig. 10(b)). In the cyclic voltammogram, redox peaks attributed to intercalation/deintercalation of Li ion into/from LiCoO<sub>2</sub> cathode were distinctively observed, indicating that the cell can be operated successfully even after one year. Observed reduction of redox current after preservation would be due to degradation of Li metal anode by reaction with small amount of CO<sub>2</sub> and/or H<sub>2</sub>O in the globe box. It can be said that the interfaces at LiCoO<sub>2</sub>/Al<sub>2</sub>O<sub>3</sub>-added LLZ and Al<sub>2</sub>O<sub>3</sub>-added LLZ/Li are very stable.

#### 4. Discussion

In this paper, an effect of Al<sub>2</sub>O<sub>3</sub> addition as the sintering additive on LLZ preparation and electrochemical properties of Al<sub>2</sub>O<sub>3</sub>-added LLZ were examined.

By the Al<sub>2</sub>O<sub>3</sub> addition, sintered LLZ could be obtained after calcination at 1000 °C. This sintering temperature was 230 °C lower than that without Al<sub>2</sub>O<sub>3</sub> addition. Any diffraction peaks for Al<sub>2</sub>O<sub>3</sub> was not observed. The Al<sub>2</sub>O<sub>3</sub> was thought to widely disperse as a small particle that cannot be detected by XRD.

Li ion conductivity and activation energy of the Al<sub>2</sub>O<sub>3</sub>-added LLZ were comparable with reported LLZ without Al<sub>2</sub>O<sub>3</sub> addition [10]. This makes us image that mechanism for Li ion conduction in the LLZ pellet was not affected by the Al<sub>2</sub>O<sub>3</sub> addition. Additionally, lithium ion could be transferred through the Al<sub>2</sub>O<sub>3</sub>-added LLZ electrolyte without any degradation of LLZ. Therefore, it can be



stated that  $\text{Al}_2\text{O}_3$  addition did not affect on stability of LLZ against Li metal.

All-solid-state battery with Li metal anode using  $\text{Al}_2\text{O}_3$ -added LLZ solid electrolyte was fabricated by using  $\text{LiCoO}_2$  cathode. In cyclic voltammogram, clear redox peaks were observed, indicating that successful operation of the all-solid-state battery with Li metal anode was achieved. Moreover, it is thought that interfaces of  $\text{Al}_2\text{O}_3$ -added LLZ/ $\text{LiCoO}_2$  and  $\text{Al}_2\text{O}_3$ -added LLZ/Li are very stable because the cell still revealed the redox properties even after one year storage in the Ar-filled globe-box. It can be inferred that the  $\text{Al}_2\text{O}_3$ -added LLZ electrolyte would be a promising candidate for all-solid-state battery because of facile preparation by the  $\text{Al}_2\text{O}_3$  addition, relatively high Li ion conductivity, and good stability against Li metal and  $\text{LiCoO}_2$  cathode. However, current density of the all-solid-state battery was quite small compared with present lithium ion battery using organic liquid electrolyte. This is due to small amount of cathode material with only 3  $\mu\text{m}$ -thickness. Additionally, it can be said that a poor contact between solid electrode and solid electrolyte would be a reason of this small current density [21]. To obtain better contact, three dimensional (3D) battery which can provide large solid–solid contact area is very useful [21–23]. We have fabricated the all-solid-state 3D battery with 3 dimensionally ordered macroporous (3DOM) structure [24]. The battery composed of  $\text{LiMn}_2\text{O}_4$  cathode and  $\text{Li}_{0.35}\text{La}_{0.55}\text{TiO}_3$  solid electrolyte provided quite large discharge capacity as all-solid-state battery, 83  $\text{mA h g}^{-1}$ . This is 56% of theoretical capacity [25]. Accordingly, higher performance of all-solid-state battery with Li metal anode would be achieved by using 3DOM  $\text{Al}_2\text{O}_3$ -added LLZ electrolyte.

Fabrication of all-solid-state battery using 3DOM  $\text{Al}_2\text{O}_3$ -added LLZ electrolyte is going on in our laboratory. New findings will be reported soon.

## 5. Conclusions

By  $\text{Al}_2\text{O}_3$  addition to  $\text{Li}_7\text{La}_3\text{Zr}_2\text{O}_{12}$  (LLZ), sintered LLZ pellet could be obtained after calcination at 1000 °C, which was 230 °C lower than that without  $\text{Al}_2\text{O}_3$  addition. This low sintering temperature leads to suppress formation of  $\text{La}_2\text{Zr}_2\text{O}_7$  impurity phase and easy preparation of LLZ ceramics electrolyte. Chemical and electrochemical properties of the  $\text{Al}_2\text{O}_3$ -added LLZ, such as stability against Li metal and ion conductivity, were comparable with the LLZ without  $\text{Al}_2\text{O}_3$  addition. Successful operation of the all-solid-state Li battery composed of Li/LLZ/ $\text{LiCoO}_2$  configuration was achieved using

the  $\text{Al}_2\text{O}_3$ -added LLZ electrolyte and the battery still worked as rechargeable battery even after one year storage in the Ar-filled globe-box. It can be inferred that the  $\text{Al}_2\text{O}_3$ -added LLZ electrolyte would be a promising candidate for all-solid-state battery because of facile preparation by the  $\text{Al}_2\text{O}_3$  addition, relatively high Li ion conductivity, and good stability against Li metal and  $\text{LiCoO}_2$  cathode. Although current density of fabricated battery was very small due to thin film cathode and poor solid–solid contact, possible fabrication and operation of all-solid-state battery with Li metal anode were clearly proven. To improve the performance of the battery, 3 dimensional structure is required.

## References

- [1] B. Scrosati, J. Garche, *J. Power Sources* 195 (2010) 2419.
- [2] F. Croce, G.B. Appetecchi, L. Persi, B. Scrosati, *Nature* 394 (1998) 456.
- [3] J.M. Tarascon, M. Armand, *Nature* 414 (2001) 359–367.
- [4] J.P. Zheng, R.Y. Liang, M. Hendrickson, E.J. Plichta, *J. Electrochem. Soc.* 155 (6) (2008) A432.
- [5] H. Fujimoto, A. Mabuchi, K. Tokumitsu, N. Chinnasamy, T. Kasuh, *J. Power Sources* 196 (2011) 1365.
- [6] B. Kumar, J. Kumar, R. Leese, J.P. Fellner, S.J. Rodrigues, K.M. Abraham, *J. Electrochem. Soc.* 157 (1) (2010) A50.
- [7] X. Xu, Z. Wen, J. Wu, X. Yang, *Solid State Ionics* 178 (2007) 2.
- [8] J.B. Bates, N.J. Nudney, B. Neudecker, A. Ueda, C.D. Evans, *Solid State Ionics* 135 (2000) 33.
- [9] P. Knauth, *Solid State Ionics* 180 (2009) 911.
- [10] R. Murugan, V. Thangadurai, W. Weppner, *Angew. Chem. Int. Ed.* 46 (2007) 7778.
- [11] M. Kotobuki, H. Munakata, K. Kanamura, Y. Sato, T. Yoshida, *J. Electrochem. Soc.* 157 (10) (2010) A1076.
- [12] V. Thangadurai, R.A. Huggins, W. Weppner, *J. Power Sources* 108 (2002) 64.
- [13] V. Thangadurai, H. Kaack, W. Weppner, *J. Am. Ceram. Soc.* 86 (2003) 437.
- [14] V. Thangadurai, W. Weppner, *J. Am. Ceram. Soc.* 88 (2005) 411.
- [15] V. Thangadurai, W. Weppner, *J. Solid State Chem.* 179 (2006) 974.
- [16] V. Thangadurai, W. Weppner, *Adv. Funct. Mater.* 15 (2005) 107.
- [17] V. Thangadurai, W. Weppner, *J. Power Source* 142 (2005) 339.
- [18] J. Fu, Y. Bai, C. Liu, H. Yu, Y. Mo, *Mater. Chem. Phys.* 115 (2009) 105.
- [19] E. Antolini, *Solid State Ionics* 170 (2004) 159.
- [20] M. Kotobuki, T. Sugiura, J. Sugaya, H. Munakata, K. Kanamura, *Electrochemistry* 78 (2010) 273.
- [21] M. Kotobuki, Y. Isshiki, H. Munakata, K. Kanamura, *Electrochim. Acta* 55 (2010) 6892.
- [22] M. Kotobuki, Y. Suzuki, H. Munakata, K. Kanamura, Y. Sato, K. Yamamoto, T. Yoshida, *J. Power Sources* 195 (2010) 5784.
- [23] M. Kotobuki, Y. Suzuki, H. Munakata, K. Kanamura, Y. Sato, K. Yamamoto, J. Yoshida, *Electrochem. Soc.* 157 (4) (2010) A493.
- [24] M. Hara, H. Nakano, D. Dokko, S. Okuda, A. Kaeriyama, K. Kanamura, *J. Power Sources* 189 (2009) 485.
- [25] R.K. Katiyara, R. Singhal, K. Asmarb, R. Valentina, R.S. Katiyarb, *J. Power Sources* 194 (2009) 526.